JOURNAL OF SOLID STATE CHEMISTRY 20, 381–389 (1977)

A Study of the Perovskite Solid Solution Series $La_xSr_{1-x}RuO_3$ and $La_xCa_{1-x}RuO_3$ by Ruthenium-99 Mössbauer Spectroscopy

FERNANDA M. DA COSTA, ROBERT GREATREX, AND NORMAN N. GREENWOOD*

Department of Inorganic and Structural Chemistry, The University of Leeds, Leeds LS2 9JT, England

Received November 18, 1976

The magnetic, electronic, and structural properties of the solid solutions $La_xSr_{1-x}RuO_3$ and $La_xCa_{1-x}RuO_3$ have been studied by ^{99}Ru Mössbauer spectroscopy and other techniques. The $La_xCa_{1-x}RuO_3$ phases are reported for the first time and have been shown by powder X-ray diffraction measurements to be orthorhombically distorted perovskites. Electrical resistivity measurements on compacted powders show that all the phases are metallic with $\rho \sim 10^{-3}$ ohm-cm. Progressive substitution of Sr^{2+} by La^{3+} in ferromagnetic $SrRuO_3$ leads to a rapid collapse of the magnetic hyperfine splitting at 4.2°K. For $x = 0.25$ some ruthenium ions still experience a magnetic field but for $0.4 \leqslant x \leqslant 0.75$ only single, narrow resonance lines are observed, consistent both with the complete removal of the ferromagnetism and with the presence of an averaged ruthenium oxidation state in each phase, i.e., $La_x^{3+}Sr_{1-x}^{2+}Ru^{(4-x)+}O_3$ rather than $La_x^{3+}Sr_{1-x}^{2+}Ru_x^{3+}Ru_{1-x}^{4+}O_3$. $LaRuO_3$ and $CaRuO_3$ both give essentially single-line spectra at 4.2°K, indicating that the ruthenium ions in these oxides are not involved in long-range antiferromagnetic order but are paramagnetic. The solid solutions $La_xCa_{1-x}RuO_3$ $(0 < x \leqslant 0.6)$ give sharp symmetrical singlets with chemical isomer shifts (relative to the Ru metal) which move progressively from the value characteristic of Ru^{4+} (−0.303 mm sec^{-1}) toward the value for Ru^{3+} (−0.557 mm sec^{-1}), consistent with the presence of intermediate ruthenium oxidation states in these phases also.

Introduction

We have recently used ^{99}Ru Mössbauer spectroscopy to examine the electronic and magnetic properties of the metallic perovskites $SrRuO_3$ (*1*, *2*), $CaRuO_3$ (*2*), and a number of solid solution phases derived from them, e.g., $SrIr_xRu_{1-x}O_3$ (*2*), $SrMn_xRu_{1-x}O_3$ (*2*), $Ca_xSr_{1-x}RuO_3$ (*3*), and $SrFe_xRu_{1-x}O_{3-y}$ (*4*). The compound $SrRuO_3$ was shown to give a well-resolved magnetic hyperfine pattern at 4.2°K, consistent with its known (*5*) ferromagnetic properties, whereas $CaRuO_3$ gave only a single sharp resonance line, indicative of paramagnetic rather than the reported (*6*) antiferromagnetic behavior.

In seeking to extend this work on mixed ruthenium oxides with the perovskite structure, the series $La_xSr_{1-x}RuO_3$ attracted our attention. This series was first studied by Bouchard and Weiher (*7*) to examine the effects on the magnetic and electrical properties of $SrRuO_3$, caused by replacing Sr^{2+} by the more highly charged La^{3+} ion. Mössbauer spectroscopy has the advantage over conventional magnetic techniques of allowing the ruthenium ions to be examined independently of other species present. In this series it should therefore be possible not only to assess the extent to which the ruthenium ions are involved in long-range magnetic order, but also to decide whether their oxidation states are discrete (Ru^{3+} and Ru^{4+}), or averaged by the formation of electronic bands or by fast electron-hopping processes.

$LaRuO_3$ itself is one of the few oxides in

* Author to whom correspondence should be addressed.

ISSN 0022-4596

which ruthenium adopts the tervalent state, the only other examples at present known being $Co^{2+}[Co^{3+}Ru^{3+}]O_4$ and $NaRu_2O_4$ (*8*). It is metallic and has been described as being antiferromagnetic, despite the absence of a clearly defined minimum in the $1/\chi$ vs T curve. This behavior was attributed to the presence of parasitic ferromagnetism, by analogy with the arguments used (incorrectly) to account for the similar magnetic behavior of $CaRuO_3$ (*7*). However, in view of our Mössbauer results on the latter, it became important to establish whether $LaRuO_3$ is in fact magnetically ordered or whether it too is paramagnetic at 4.2°K. The Mössbauer data might also be expected to throw some light on the electronic configuration of $LaRuO_3$, a topic which has been the subject of some controversy (*9*, *10*).

Our results on the $La_xSr_{1-x}RuO_3$ series have led us further to investigate the analogous substitution of lanthanum for calcium in $CaRuO_3$. The preparation of these new phases $La_xCa_{1-x}RuO_3$ and their characterization by powder X-ray diffraction are described in this paper together with the results of the Mössbauer studies. Preliminary electrical resistivity measurements on compacted powder samples of both series are also discussed.

Experimental

$CaRuO_3$ and $SrRuO_3$ were prepared by heating the appropriate alkaline earth carbonate and ruthenium metal in air at 1100°C using published methods (*11*, *12*). $LaRuO_3$ was prepared by heating a pelleted mixture of La_2O_3, RuO_2, and ruthenium metal in an evacuated, sealed platinum tube of a diameter of 5 mm and a wall thickness of 0.25 mm at temperatures up to 1350°C using the method of Bouchard and Weiher (*7*). The solid solutions $La_xSr_{1-x}RuO_3$ ($x = 0.1$, 0.25, 0.4, 0.5, 0.55, 0.6, and 0.75) and $La_xCa_{1-x}RuO_3$ ($x = 0.2$, 0.4, 0.5, and 0.6) were prepared by the same method from either $SrRuO_3$ or $CaRuO_3$ and the components of $LaRuO_3$ (La_2O_3, RuO_2, and Ru) mixed in the appropriate proportions. The tubes and their contents were weighed carefully before and after being heated to check the integrity of the seal, and they were weighed again, after opening, to check for loss or uptake of oxygen. No significant weight changes were observed. Loss of small amounts of ruthenium by diffusion into the walls of the platinum tube may have occurred but the X-ray diffraction data presented in the following section show no evidence that the desired stoichiometry had not been achieved. Several attempts were made to prepare samples of $La_xCa_{1-x}RuO_3$ with compositions in the range $0.6 < x < 1.0$, but the products were shown by their X-ray powder patterns always to contain small amounts of unidentified phases in addition to the perovskite phase.

A Philips powder diffractometer employing Cu$K\alpha$ radiation ($\lambda = 154.18$ pm) was used to characterize the phases, and cell dimensions were derived from least-squares refinement of the d values. Electrical resistivity was measured on compacted powder samples at room temperature, 77°K, and 4.2°K, using a four-probe technique. Cryogenic temperatures were achieved by immersing a specially designed cell in either liquid nitrogen or liquid helium. The ^{99}Ru Mössbauer spectra were recorded at 4.2°K using techniques described previously (*3*). Several radioactive sources were used and their experimental linewidths, Γ, measured using natural ruthenium metal as an absorber (100 mg cm^{-2}), were in the range 0.25–0.36 mm sec^{-1}. Further information about the source used in a particular experiment is given in the Tables.

Crystallographic Data

The materials were shown to be single-phase orthorhombic perovskites belonging to the space group *Pbnm* typified by $GdFeO_3$ (Fig. 1) (*13*, *14*). No reflections from a supercell were detected for any of the phases studied, but in view of the recent electron diffraction studies of Gai and Rao (*15*) this may not be sufficient evidence by itself to rule out cation ordering; their data revealed a doubling of the unit cell in $La_{0.5}Sr_{0.5}CoO_3$, that could not be detected in the Debye–Scherrer or Guinier patterns.

For the phases $La_xSr_{1-x}RuO_3$ the reflections in the X-ray powder patterns could all be indexed satisfactorily using the cell dimensions

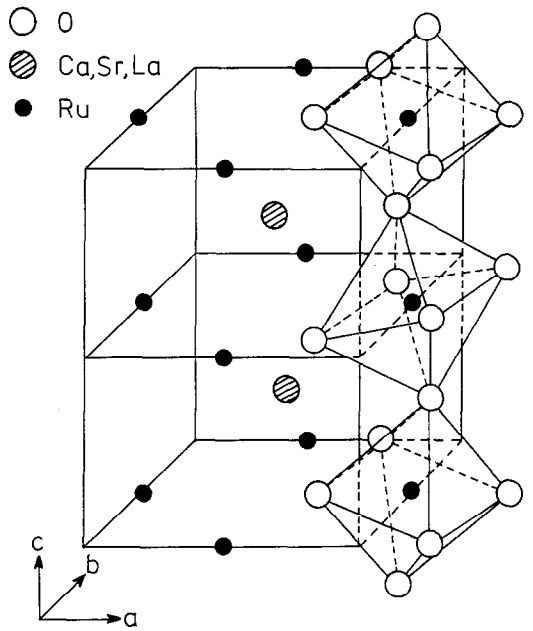

FIG. 1. Part of the orthorhombic unit cell of $GdFeO_3$, showing how the MO_6 octahedra are tilted about the b and c axes.

quoted by Bouchard and Weiher (*7*). As these authors have pointed out, there is a small but regular increase in the cell volume with increasing x indicating that the effect of substituting the larger Ru^{3+} (68 pm) for Ru^{4+} (62 pm) in the B sublattice of the ABO_3 perovskite structure is dominant over the effect of substituting the smaller La^{3+} (118 pm) for Sr^{2+} (125 pm); the ionic radii are those quoted by Shannon and Prewitt for the sixfold B-ion and eightfold A-ion-coordination (*16*). Although the cell volume increases regularly with x, the cell dimensions a, b, and c show differing dependences. Thus, a and c go through a maximum and there is a crossover from $a > b$ to $a < b$ at $x \sim 0.5$, where the phase is essentially cubic. The b dimension does not go through a maximum, but instead continues to increase for $x > 0.5$. The rate of increase becomes very rapid at high x and this led Bouchard and Weiher to suggest that a factor other than size considerations may be important in determining the trends in the cell volume. As a result of these variations $LaRuO_3$ is much more distorted from cubic symmetry than $SrRuO_3$. The probable effect of the orthorhombic distortion is to tilt the RuO_6 octahedra about the b and c axes as illustrated in Fig. 1 for the idealized $GdFeO_3$ structure, and this may have important implications regarding the superexchange interactions in these phases. It is also important to note that although the oxygen environment of the large A cation is considerably distorted, the BO_6 octahedra remain almost regular in the $GdFeO_3$-type structure (*13*, *14*).

For the series $La_xCa_{1-x}RuO_3$ the refined cell dimensions (in picometers) and cell volumes (in cubic nanometers), as a function of x, are listed in Table I and illustrated in Fig. 2. As La^{3+} (118 pm) replaces Ca^{2+} (112 pm) in $CaRuO_3$ the radii of both the A and B cation increase simultaneously, and as might

TABLE I

REFINED CELL DIMENSIONS AND CELL VOLUMES FOR THE PHASES $La_xCa_{1-x}RuO_3$[a]

Phase	a(pm)	b(pm)	c(pm)	V(nm^3)
$CaRuO_3$	534.4(4)	550.0(3)	763.7(7)	0.2245(5)
$La_{0.2}Ca_{0.8}RuO_3$	538.4(2)	554.3(2)	768.7(3)	0.2294(3)
$La_{0.4}Ca_{0.6}RuO_3$	542.3(4)	557.5(4)	774.0(6)	0.2340(5)
$La_{0.5}Ca_{0.5}RuO_3$	544.9(3)	560.3(4)	777.6(5)	0.2374(5)
$La_{0.6}Ca_{0.4}RuO_3$	546.1(3)	561.5(3)	778.3(4)	0.2387(4)
$LaRuO_3$	548.9(3)	574.8(2)	784.5(3)	0.2475(3)

[a] The numbers in parentheses are the standard deviations in the last significant figure, and do not include any effects caused by systematic errors. The latter were minimized by the use of an internal silicon standard.

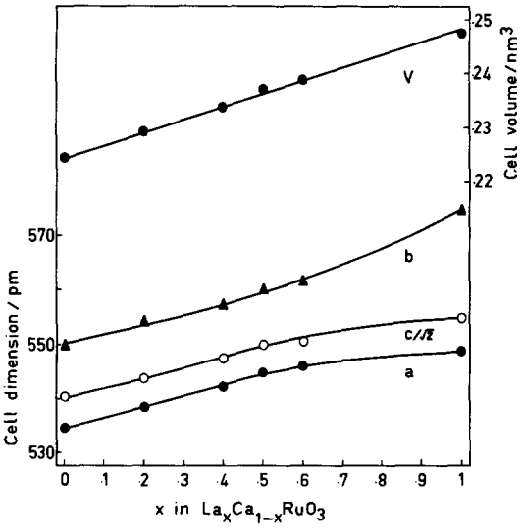

FIG. 2. The variations in cell dimensions and cell volume with composition for the series $La_xCa_{1-x}RuO_3$.

therefore have been expected a regular increase in the cell volume occurs. The individual cell dimensions also vary smoothly across the series and there is no unusual crossover of the type exhibited by the $La_xSr_{1-x}RuO_3$ series.

Electrical Resistivity

Electrical resistivities of compacted powder samples at room temperature, 77°K, and 4.2°K are recorded in Table II. These values are likely to be higher than those obtainable from single crystals; for example, measurements on single crystals of $CaRuO_3$ and $SrRuO_3$ have given values of 2.5×10^{-4} and 2.8×10^{-4} ohm-cm, respectively, at 300°K (*17*). Nevertheless, the data establish quite clearly that the resistivity of all the solid solutions increases with increase in temperature and is similar in magnitude to that displayed by the metallic end members. The metallic conductivity in these perovskite phases is thought to arise from the favorable overlap between the ruthenium t_{2g} and oxygen p orbitals, which generates a partially filled π^* band (*7*).

Mössbauer Measurements

The End-Members $SrRuO_3$, $CaRuO_3$, and $LaRuO_3$

The Mössbauer spectra of $SrRuO_3$ and $CaRuO_3$ at 4.2°K have been published previously (*1*, *2*). $SrRuO_3$ gave an 18-line pattern due to the magnetic splitting of the $I_g = 5/2 \rightarrow I_e = 3/2$ transition in ^{99}Ru with a single hyperfine field of flux density 35.2 T (352 kG) and a chemical isomer shift of –0.325(7) mm sec^{-1}. $CaRuO_3$ gave a single resonance line with a linewidth of 0.40 mm sec^{-1} and a chemical isomer shift of –0.296(3) mm sec^{-1} appropriate to a paramagnetic Ru^{4+} cation on a cubic site. In the present work the spectrum of $CaRuO_3$ was re-recorded with a source of narrower linewidth (Γ 0.25 mm sec^{-1}) so that it could be compared directly with the spectra of the solid-solution series $La_xCa_{1-x}RuO_3$. The improved counting statistics and enhanced quality of the spectrum revealed that the data deviate significantly from a single Lorentzian, and are best computed as an unresolved quadrupole-split doublet with $\frac{1}{2}e^2qQ_e = 0.117(4)$ mm sec^{-1} as shown in Fig. 3. The solid line through the data points is the computed least-squares fit of two Lorentzian lines constrained to have equal linewidths. The intensities emerge in the ratio 1:1 and the linewidth of 0.274(6) mm sec^{-1} is almost identical with that obtained using the same source in conjunction with a ruthenium metal (single-line) absorber.

TABLE II

ELECTRICAL RESISTIVITIES FOR COMPACTED POWDER SAMPLES OF THE PHASES $La_xSr_{1-x}RuO_3$ AND $La_xCa_{1-x}RuO_3$

Phase	Electrical resistivity $\rho/(10^{-3}$ ohm-cm)		
	$T = 4.2$°K	$T = 77$°K	$T = 300$°K
$LaRuO_3$	1.08	1.20	1.74
$SrRuO_3$	0.22	0.64	0.89
$CaRuO_3$	0.04	0.07	0.23
$La_{0.1}Sr_{0.9}RuO_3$	0.28	0.69	0.94
$La_{0.25}Sr_{0.75}RuO_3$	0.34	0.76	1.15
$La_{0.4}Sr_{0.6}RuO_3$	0.44	0.88	1.91
$La_{0.5}Sr_{0.5}RuO_3$	0.71	1.35	3.11
$La_{0.6}Sr_{0.4}RuO_3$	1.23	1.82	4.00
$La_{0.2}Ca_{0.8}RuO_3$	0.10	0.16	0.17
$La_{0.4}Ca_{0.6}RuO_3$	0.21	0.40	0.67
$La_{0.5}Ca_{0.5}RuO_3$	0.22	0.37	0.94
$La_{0.6}Ca_{0.4}RuO_3$	0.31	0.87	1.99

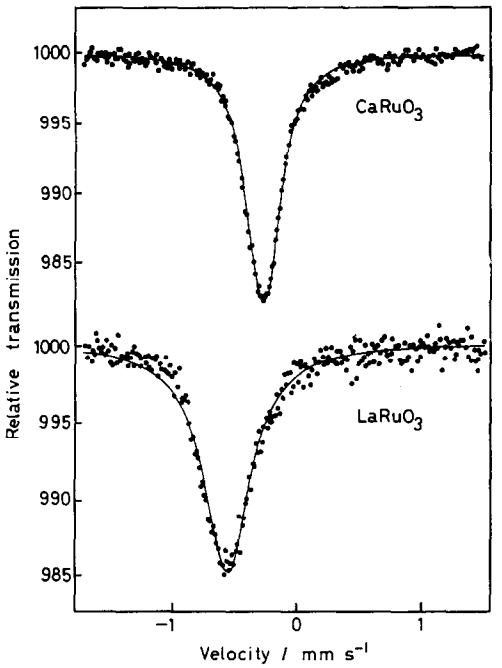

FIG. 3. Ruthenium-99 Mössbauer spectra at 4.2°K for $CaRuO_3$ and $LaRuO_3$. The values of the baseline are 6.43×10^6 and 3.13×10^6 counts per channel, respectively.

The Mössbauer spectrum of $LaRuO_3$ also consists essentially of a single line as shown in Fig. 3 though the resonance line is broader than that of $CaRuO_3$. A slight quadrupole splitting may be present but no attempt has been made to fit this. The lack of substantial quadrupole splitting in the spectra of both $CaRuO_3$ and $LaRuO_3$ implies that the large orthorhombic distortion in these perovskites occurs in such a way as to leave the RuO_6 octahedra almost regular, as discussed under Crystallographic Data.

The Mössbauer parameters for $SrRuO_3$, $CaRuO_3$, and $LaRuO_3$ are summarized in Table III, together with data for a selection of other ruthenium oxides, showing that the three oxidation states Ru^{3+}, Ru^{4+}, and Ru^{5+} are readily distinguishable in oxide systems on the basis of their chemical isomer shifts. The value for $LaRuO_3$, −0.557(3) mm sec^{-1}, is almost identical with that for the spinel Co_2RuO_4 which is one of the few known examples of Ru^{3+} in an oxide lattice. It is difficult to reconcile this with Goodenough's model for $LaRuO_3$ in which four electrons are localized on the t_{2g} orbitals of Ru^{4+}, with the fifth

TABLE III

MÖSSBAUER PARAMETERS AT 4.2°K FOR THE PEROVSKITES $MRuO_3$ (M = Ca, Sr, AND La) AND OTHER OXIDE PHASES CONTAINING Ru^{3+}, Ru^{4+}, AND Ru^{5+}

Phase	Chemical isomer shift[a] δ/mm sec^{-1}	Quadrupole splitting $\frac{1}{2}e^2qQ_e$/mm sec^{-1}	Magnetic flux density B/T	Linewidth Γ/mm sec^{-1}	Reference
$SrRu^{4+}O_3$	−0.325(7)[b]	0	35.2(1.5)	0.43(2)	2
$CaRu^{4+}O_3$	−0.300(3)	0.117(4)[c]	0	0.274(6)	This work
$LaRu^{3+}O_3$	−0.557(3)	0	0	0.454(5)	This work
$Co_2Ru^{3+}O_4$	−0.567(1)	−0.728(10)	0	0.269(4)	8
$Ru^{4+}O_2$	−0.23(1)	−0.696(19)	0	0.57(3)	—[d]
$BaRu^{4+}O_3$	−0.257(5)	0	0	0.40(2)	2
$Y_2Ru_2^{4+}O_7$	−0.226(19)	0	12.6(8)	0.43	2
$Sr_2Ru^{4+}O_4$	−0.279(2)	0	0	0.293(5)	—[e]
$Sr_2Fe^{3+}Ru^{5+}O_6$	+0.116(38)	0	52.9(7)	0.74(9)	4
$Na_3Ru^{5+}O_4$	+0.110	0	58.7(1.2)	0.31(1)	8

[a] Relative to ruthenium metal.

[b] The numbers in the parentheses are the standard deviations in the last significant figure.

[c] Sign not determined.

[d] D. C. Foyt, J. G. Cosgrove, R. L. Collins, and M. L. Good, *J. Inorg. Nuclear Chem.* 37, 1913 (1975).

[e] R. Greatrex, N. N. Greenwood, and K. G. Snowdon, unpublished data.

electron being delocalized into a σ^* band (*10*). The observed chemical isomer shift implies a configuration much nearer to Ru^{3+}, with very little delocalization into the conduction band. Moreover, the complete absence of magnetic hyperfine splitting in the spectrum of $LaRuO_3$ indicates that, as in $CaRuO_3$, there is no long-range antiferromagnetic order and that the material is paramagnetic at 4.2°K. This is contrary to the suggestion (*7*), that $LaRuO_3$ is antiferromagnetic with parasitic ferromagnetism. Such magnetic ordering of Ru^{3+} would generate a flux density of ca. 17.6 T, and this would be readily observable as a substantial line broadening of at least 2 mm sec^{-1} in the Mössbauer spectrum (*3*, *4*).

The Series $La_xSr_{1-x}RuO_3$

Mössbauer spectra have been recorded for the series $La_xSr_{1-x}RuO_3$ ($x = 0.1$, 0.25, 0.4, 0.5, 0.55, 0.6, 0.65, and 0.75) and representative examples are shown in Figs. 4 and 5, which reveal that progressive substitution of Sr^{2+} by La^{3+} leads rapidly to the collapse of the magnetic splitting. The partially collapsed spectra have not been analyzed by computer curve-fitting techniques, but visual inspection indicates that for $x = 0.1$ the total width of the resonance at half maximum height is ca. 3.1 mm sec^{-1}, corresponding to a magnetic flux density of 25.3 T. This can be compared with a flux density of 35.2 T for the parent $SrRuO_3$. The chemical isomer shift for this phase is ca. −0.33 mm sec^{-1}. The sample with 25% La^{3+} still shows a residual magnetic splitting (Fig. 4) but $La_{0.4}Sr_{0.6}RuO_3$ has only a sharp resonance line (Fig. 5). This is entirely consistent with the magnetic susceptibility data of Bouchard and Weiher (*7*), which indicate that the ferromagnetism present in $SrRuO_3$ disappears at ca. 35% La^{3+}.

Similar inward collapse of the spectrum was observed in our earlier measurements (*3*) on the phase $Ca_xSr_{1-x}RuO_3$, the sharp "paramagnetic" component present in the spectra of samples with $x > 0.3$ being attributed to weakly coupled ruthenium ions undergoing rapid electronic relaxation. However, even in samples containing as much as 50% Ca^{2+}, a few of the ruthenium ions still experienced

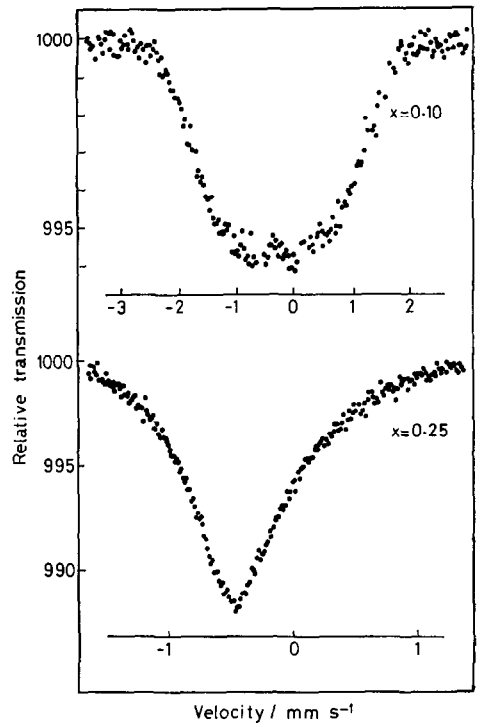

FIG. 4. Ruthenium-99 Mössbauer spectra at 4.2°K for $La_{0.1}Sr_{0.9}RuO_3$ and $La_{0.25}Sr_{0.75}RuO_3$. The values of the baseline are 18.5×10^6 and 16.9×10^6 counts per channel, respectively.

substantial magnetic flux densities (*3*). The present results therefore suggest that La^{3+} is more effective than Ca^{2+} in breaking down the superexchange interaction responsible for the ferromagnetism. In seeking to explain this we note first that the magnetic flux density for the low-spin d^5 Ru^{3+} ion, which contains one unpaired electron, is expected to be ca. 17.6 T (*4*) compared with ca. 35.2 T for Ru^{4+} which has two unpaired electrons. This will lead to an apparently more rapid collapse of the magnetic splitting but is by itself insufficient to account for the observed behavior. Of greater importance is the higher charge and smaller size of La^{3+} compared with Sr^{2+} which enable it to compete even more strongly for the oxygen electrons than does Ca^{2+} in the $Ca_xSr_{1-x}RuO_3$ series. In addition, as Bouchard and Weiher have pointed out (*7*), the Ru^{3+} ions resulting from the substitution

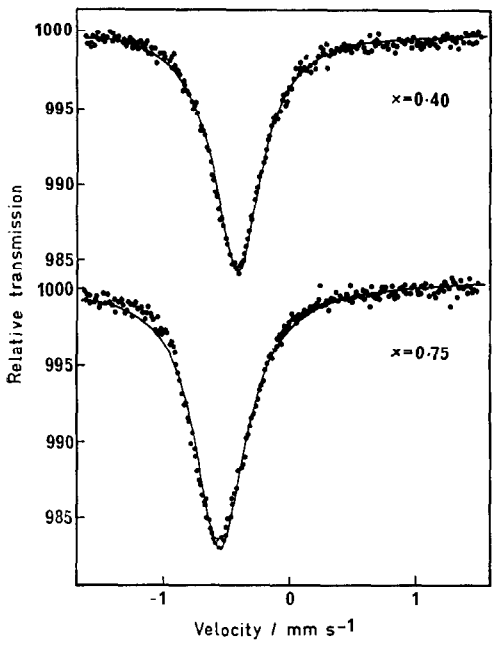

FIG. 5. Ruthenium-99 Mössbauer spectra at 4.2°K for $La_xSr_{1-x}RuO_3$ ($x = 0.40$ and 0.75). The values of the baseline are 7.88×10^6 and 9.98×10^6 counts per channel, respectively.

are less strongly bonded than the Ru^{4+}. The net result is that the Ru–O–Ru magnetic superexchange interaction is so severely weakened that the long-range magnetic order present in $SrRuO_3$ collapses entirely with the introduction of only ca. 35% La^{3+}.

In a recent paper Takano et al. have reported that the magnetic flux densities at diamagnetic $^{119}Sn^{4+}$ nuclei in the antiferromagnetic phases $Ca_xSr_{1-x}Mn_{0.99}Sn_{0.01}O_3$ depend linearly upon the numbers of Ca^{2+} and Sr^{2+} ions in the neighbouring divalent cation sites, with proportional coefficients having opposite signs (*18*). Their results were discussed in terms of two spin transfer processes: a metal–oxygen–metal interaction and an interaction via the A^{2+} cations, which becomes dominant in the strontium-rich phases. Although interactions via the divalent cations may also be important in the ruthenium systems, it would be unwise to draw parallels, especially as the spin states of the ions involved are quite different.

We have not attempted to analyze the partially collapsed $La_xSr_{1-x}RuO_3$ spectra in more detail because the problem is now even more complex than that encountered in the $Ca_xSr_{1-x}RuO_3$ system, owing to the additional possibility of ruthenium being present in more than one oxidation state. In this respect it is perhaps significant that the spectra are somewhat asymmetric. The spectrum for the sample with $x = 0.25$ in particular appears to consist of a broadened singlet, centered at ca. –0.48 mm sec^{-1}, superimposed on a broader magnetic background which is displaced towards a more positive velocity of ca. –0.32 mm sec^{-1}. This may reflect a tendency for the ruthenium ions to be present as Ru^{3+} in paramagnetic La^{3+}-rich regions and Ru^{4+} in ferromagnetic Sr^{2+}-rich regions, although a model in which the electrons are completely localized is ruled out by the metallic conductivity of the phases. Further work on this system, at temperatures above the Curie point, might give a more detailed indication of the ruthenium oxidation states involved.

For samples containing between 40 and 75% La^{3+} ($0.4 \leqslant x \leqslant 0.75$) the Mössbauer spectra consist of symmetrical single lines (Fig. 5). These have been curve fitted with single Lorentzians and the resulting chemical isomer shifts and linewidths are listed in Table IV.

TABLE IV

MÖSSBAUER PARAMETERS AT 4.2°K FOR THE SOLID SOLUTIONS $La_xSr_{1-x}RuO_3$ ($0.4 \leqslant x \leqslant 0.75$)[a]

Phase	Chemical isomer shift[b] δ/mm sec^{-1}	Linewidth Γ/mm sec^{-1}	χ^2/degrees of freedom
$La_{0.4}Sr_{0.6}RuO_3$[c]	–0.468(1)	0.451(5)	233/246
$La_{0.5}Sr_{0.5}RuO_3$[c]	–0.426(2)	0.495(9)	227/246
$La_{0.55}Sr_{0.45}RuO_3$[d]	–0.480(3)	0.412(11)	241/246
$La_{0.6}Sr_{0.4}RuO_3$[d]	–0.454(4)	0.459(14)	259/246
$La_{0.65}Sr_{0.35}RuO_3$[d]	–0.454(4)	0.523(2)	237/246
$La_{0.75}Sr_{0.25}RuO_3$[e]	–0.499(2)	0.413(6)	619/246

[a] Values for the end members are given in Table I and those for $x = 0.1$ and 0.25 are discussed in the text.
[b] Relative to ruthenium metal.
[c] Recorded with a source of experimental line width $\Gamma = 0.36$ mm sec^{-1} using a ruthenium-metal absorber.
[d] Source vs Ru metal $\Gamma = 0.32$ mm sec^{-1}.
[e] Source vs Ru metal $\Gamma = 0.25$ mm sec^{-1}.

The linewidths are rather large but this is due mainly to the broadened emission line for the source used. The chemical isomer shifts are all intermediate between the values characteristic of Ru^{3+} and Ru^{4+} (–0.56 and –0.30 mm sec^{-1}, respectively, see Table III), and are therefore consistent with the presence of ruthenium in an intermediate oxidation state. The phases are accordingly better formulated as $La_xSr_{1-x}Ru^{(4-x)+}O_3$ rather than $La_xSr_{1-x}Ru_x^{3+}Ru_{1-x}^{4+}O_3$. In this respect the series resembles the systems $La_xSr_{1-x}FeO_{3-y}$ (*19*) and $La_xSr_{1-x}CoO_3$ (*20*) for which Mössbauer spectra are consistent with the presence of intermediate oxidation states for the transition metal.

The Series $La_xCa_{1-x}RuO_3$

Mössbauer spectra at 4.2°K for the series $La_xCa_{1-x}RuO_3$ ($x = 0.2$, 0.4, 0.5, and 0.6) are shown in Fig. 6. The spectra consist of single narrow resonance lines with no complications arising from magnetic interactions. The solid lines through the data points are the computed least-squares fits to single Lorentzian lines, and the corresponding parameters are listed in Table V. The chemical isomer shifts move gradually and proportionately between the values typical for Ru^{4+} in $CaRuO_3$ and Ru^{3+} in $LaRuO_3$. The data are therefore consistent with the presence of an intermediate oxidation state for ruthenium in these phases. The linewidths, which lie in the range 0.34–0.45 mm sec^{-1}, are comparable with that for $CaRuO_3$ itself (0.33 mm sec^{-1}), the slight additional broadening being due to the range of ruthenium environments resulting from the statistical distribution of Ca^{2+} and La^{3+} cations on the *A* sites. Careful inspection of Fig. 6 shows that the lineshapes are not truly Lorentzian, and this results in the rather high χ^2 values given in Table V. However, the resonance lines are symmetrical about their centroids and show no evidence for the two absorption peaks of unequal intensity that would be implied by a formulation involving discrete ruthenium oxidation states, i.e., $La_x^{3+}Ca_{1-x}^{2+}Ru_x^{3+}Ru_{1-x}^{4+}O_3$.

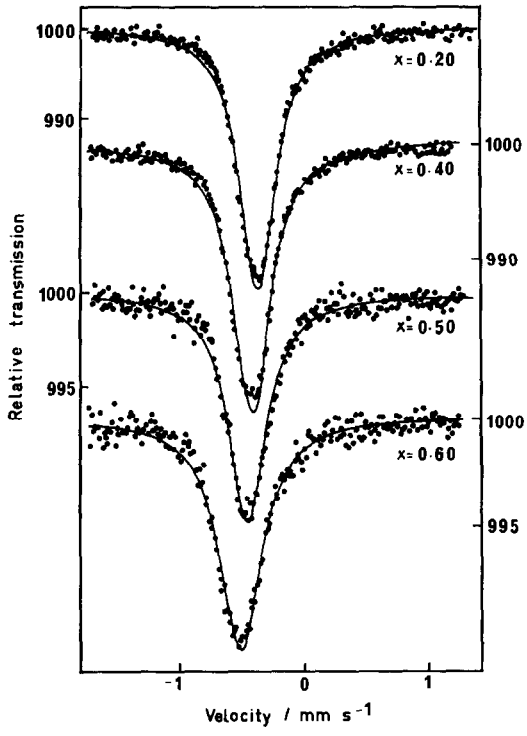

FIG. 6. Ruthenium-99 Mössbauer spectra at 4.2°K for $La_xCa_{1-x}RuO_3$ ($x = 0.20$, 0.40, 0.50, and 0.60). The values of the baseline are 4.26×10^6, 7.18×10^6, 4.99×10^6, and 6.07×10^6 counts per channel, respectively.

TABLE V

MÖSSBAUER PARAMETERS AT 4.2°K FOR SINGLE-LINE FITS TO THE SPECTRA[a] FOR $La_xCa_{1-x}RuO_3$ ($x = 0$, 0.2, 0.4, 0.5, 0.6, and 1.0)

Phase	Chemical isomer shift δ/mm sec^{-1}	Linewidth Γ/mm sec^{-1}	χ^2/degrees of freedom
$CaRuO_3$	–0.303(2)	0.331(4)	239/246
$La_{0.2}Ca_{0.8}RuO_3$	–0.369(1)	0.345(4)	521/246
$La_{0.4}Ca_{0.6}RuO_3$	–0.431(2)	0.362(5)	576/246
$La_{0.5}Ca_{0.5}RuO_3$	–0.466(2)	0.374(8)	300/246
$La_{0.6}Ca_{0.4}RuO_3$	–0.483(3)	0.412(9)	320/246
$LaRuO_3$	–0.557(3)	0.454(5)	349/246

[a] The spectra were recorded with a source of experimental line width $\Gamma = 0.25$ mm sec^{-1} using a ruthenium metal absorber.

Conclusions

It has been shown that progressive substitution of Sr^{2+} by La^{3+} in the metallic band ferromagnet $SrRuO_3$ leads to a more rapid collapse of the magnetic hyperfine splitting than that effected by Ca^{2+} substitution in $SrRuO_3$. This behavior has been interpreted in terms of a competition between the A cations and the ruthenium ions for the oxygen electron density involved in the magnetic superexchange interaction, and the results imply that the electron-pair acceptor strength (Lewis acidity) of the A cation decreases in the order $La^{3+} > Ca^{2+} > Sr^{2+}$. For $La_xSr_{1-x}RuO_3$ ($x = 0.25$) some of the ruthenium ions still experience a magnetic field, but for $0.4 \leqslant x \leqslant 0.75$ only single narrow resonance lines are observed, consistent both with the complete removal of the ferromagnetism and with the presence of an averaged ruthenium environment in each phase, i.e., $La_x^{3+}Sr_{1-x}^{2+}Ru^{(4-x)+}O_3$ rather than $La_x^{3+}Sr_{1-x}^{2+}Ru_x^{3+}Ru_{1-x}^{4+}O_3$.

$LaRuO_3$ and $CaRuO_3$ both give essentially single-line spectra, indicating that the ruthenium ions in these oxides are not ordered antiferromagnetically but are paramagnetic. Their chemical isomer shifts are typical of Ru^{3+} and Ru^{4+} in oxide phases and are, respectively, $-0.557(3)$ and $-0.303(2)$ mm sec^{-1} relative to ruthenium metal. The solid solutions $La_xCa_{1-x}RuO_3$ ($0 < x < 0.6$), which are reported here for the first time, also give sharp symmetrical singlets with chemical isomer shifts which move gradually and proportionately between those of the end members, consistent with the presence of an averaged ruthenium oxidation state. All of the phases are metallic and have a resistivity of ca. 10^{-3} ohm-cm.

Acknowledgments

The authors thank Dr. T. C. Gibb for helpful discussions, the S.R.C. for financial support, and the Comissao Permanente INVOTAN for a grant (to F. M. D. C.).

References

1. T. C. Gibb, R. Greatrex, N. N. Greenwood, and P. Kaspi, *Chem. Commun.* p. 319 (1971).
2. T. C. Gibb, R. Greatrex, N. N. Greenwood, and P. Kaspi, *J. Chem. Soc.* (*Dalton Trans.*), p. 1253 (1973).
3. T. C. Gibb, R. Greatrex, N. N. Greenwood, D. C. Puxley, and K. G. Snowdon, *J. Solid State Chem.* **11**, 17 (1974).
4. T. C. Gibb, R. Greatrex, N. N. Greenwood, and K. G. Snowdon, *J. Solid State Chem.* **14**, 193 (1975).
5. A. Callaghan, C. W. Moeller, and R. Ward, *Inorg. Chem.* **5**, 1572 (1966).
6. J. M. Longo, P. M. Raccah, and J. B. Goodenough, *J. Appl. Phys.* **39**, 1327 (1968).
7. R. J. Bouchard and J. F. Weiher, *J. Solid State Chem.* **4**, 80 (1972).
8. T. C. Gibb, R. Greatrex, N. N. Greenwood, D. C. Puxley, and K. G. Snowdon, *Chem. Phys. Lett.* **20**, 130 (1973); N. N. Greenwood, F. M. Da Costa, and R. Greatrex, *Rev. Chim. Miner.* **13**, 133 (1976).
9. R. J. Bouchard, J. F. Weiher, and J. L. Gillson, *J. Solid State Chem.* **6**, 519 (1973).
10. J. B. Goodenough, *Mater. Res. Bull.* **6**, 967 (1971).
11. J. J. Randall and R. Ward, *J. Amer. Chem. Soc.* **81**, 2629 (1959).
12. P. C. Donahue, L. Katz, and R. Ward, *Inorg. Chem.* **4**, 306 (1965).
13. P. Coppens and M. Eibschütz, *Acta Crystallogr.* **19**, 524 (1965).
14. A. J. Jacobson, B. C. Tofield, and B. E. F. Fender, *Acta Crystallogr.* **B28**, 956 (1972).
15. P. L. Gai and C. N. R. Rao, *Mater. Res. Bull.* **10**, 787 (1975).
16. R. D. Shannon and C. T. Prewitt, *Acta Crystallogr.* **B25**, 925 (1969).
17. R. J. Bouchard and J. L. Gillson, *Mater. Res. Bull.* **7**, 873 (1972).
18. M. Takano, Y. Takeda, M. Shimada, T. Matsuzawa, T. Shinjo, and T. Takada, *J. Phys. Soc. Japan* **39**, 656 (1975).
19. U. Shimony and J. M. Knudsen, *Phys. Rev.* **144**, 361 (1966).
20. V. G. Bhide, D. S. Rajoria, C. N. R. Rao, G. Rama Rao, and V. G. Jadhao, *Phys. Rev. B.* **12**, 2832 (1975).